

# Microcantilever-Based MEMS Biosensor for Viral Pathogens

Anika Tun Naziba, Mahmudul Hoque Mahmud, Manika Tun Nafisa, S M Atiqur Rahman, Ariful Hoque Maruf, Md Tanvir Hasan and Mohammad Nasir Uddin

**Abstract**—Microcantilever-based MEMS (Micro-Electro-Mechanical Systems) sensors are rapidly emerging as powerful tools for detecting various viral diseases. This study investigates microcantilever-based MEMS sensors for detecting viral pathogens, focusing on SARS-CoV-2. Motivated by the need for rapid and efficient viral diagnostics, the pull-in voltage of various microcantilever materials is analyzed using the Finite Difference Time Domain (FDTD) method. Displacement and capacitance of microcantilevers composed of nickel, molybdenum, gold, and titanium-gold (Ti-Au) are simulated under electrostatic actuation. Results demonstrate that the Ti-Au microcantilever exhibits a lower pull-in voltage (4.978V) compared to nickel (6.55V), molybdenum (6.38V), and gold (5.26V). Furthermore, Ti-Au shows favorable capacitance and sensitivity characteristics. It is concluded that Ti-Au is a promising material for microcantilever-based MEMS biosensors due to its superior performance in terms of pull-in voltage, capacitance, and sensitivity, making it a potentially valuable component for rapid COVID-19 detection.

**Index Terms**—Microcantilever beam, COVID-19, Micro-Electromechanical System (MEMS), Pull-in voltage, Radio-Frequency (RF), Titanium Gold (Ti-Au).

## I. INTRODUCTION

**B**IOMEDICAL engineers focus on technological innovations and healthcare developments in order to create new equipment for enhancing human health and diagnosing deadly illnesses such as cancer, COVID-19, influenza, respiratory syncytial virus (RSV), hepatitis viruses, Ebola, Zika virus, etc. [1]–[14]. These viral diseases, like the recent COVID-19 pandemic, have significantly disrupted our daily lives. More than 770 million cases have been reported and more than 7 million people had died from the sickness by September 2024 [15]. Numerous countries have implemented non-therapeutic sensible precautions such as travel restrictions,

**Anika Tun Naziba**, Department of Electrical and Electronics Engineering, American International University-Bangladesh (AIUB), Dhaka, Bangladesh. Email: [anikanaziba9@gmail.com](mailto:anikanaziba9@gmail.com)

**Mahmudul Hoque Mahmud**, Department of Computer Science, American International University-Bangladesh (AIUB), Dhaka, Bangladesh. Email: [mhoque@isrt.ac.bd](mailto:mhoque@isrt.ac.bd)

**Manika Tun Nafisa**, Interdisciplinary Engineering, Kennesaw State University, Marietta, GA 30060, USA. Email: [nafisamanika@gmail.com](mailto:nafisamanika@gmail.com)

**S M Atiqur Rahman**, Interdisciplinary Engineering, Kennesaw State University, Marietta, GA 30060, USA. Email: [rahmanatiq.engr@gmail.com](mailto:rahmanatiq.engr@gmail.com)

**Ariful Hoque Maruf**, Institute of Information and Technology, University of Dhaka, Bangladesh. Email: [bsse0621@iit.du.ac.bd](mailto:bsse0621@iit.du.ac.bd)

**Md Tanvir Hasan**, Department of Electrical and Electronic Engineering, Jashore University of Science and Technology, Jashore, Bangladesh. Email: [mth@just.edu.bd](mailto:mth@just.edu.bd)

**Mohammad Nasir Uddin**, Department of Electrical and Electronics Engineering, American International University-Bangladesh (AIUB), Dhaka, Bangladesh. Email: [dmasir@aiub.edu](mailto:dmasir@aiub.edu)

remote office operations, countrywide lockdowns and most significantly, social isolation. It is transmitted by inhalation of virus-carrying microparticles in the air, as seen in Fig. 1.



Fig. 1. COVID-19 viral transmission.

Fever, cough, headache, exhaustion, breathing difficulty, absence of smell and loss of taste are common symptoms of COVID-19 [16]–[18]. COVID-19 requires quick medical attention in order to be safe in this life-threatening situation. Because of the longer treatment interval, the patient would experience more pain and suffering. If people know ahead of time that they are infected with coronavirus by any rapid medical intervention, they can engage in self-isolation to limit the spreading of the coronavirus and be able to avoid this condition through proper care and medication.

A variety of coronavirus testing methods are available, including the Reverse transcription polymerase chain reaction (RT-PCR) test, Surface plasmon resonance (SPR) test etc. RT-PCR is a nuclear-derived technique for detecting coronavirus appearance. Swab Test [19], Nasal aspirates [20], Tracheal aspirates [21], Sputum Test [22] and Blood Test [23] are all part of the RT-PCR test. According to previous reports, the outcomes of these methods are significantly dependent on sample collection time, type, storage, handling and processing. Depending on the laboratory devices and systems, coronavirus diagnosis might take 24–72 hours or 1–3 days including sample collection and report generation process [24]. The RT-PCR method's accuracy is excellent, although it is very time-consuming and expensive. It cannot be performed at home. This procedure consumes a large number of resources and generates a significant quantity of waste, which is difficult to dispose of. By producing or developing less hazardous material in the shortest amount of time, this time-consuming problem can be resolved right away. Surface plasmon resonance (SPR) is a successful method, which can be employed for easy and rapid detection of COVID-19 infection-related antigens. It is

a label-free optical method for tracking strong interaction via changes in the refractive index of the metal at the surface. In comparison to tests performed, results are obtained in 10–15 minutes [25]. During the first five days of symptoms, this testing is more precise; beyond that, it is impossible to obtain an exact result. It can be done at home, but there is another alternative way of testing that provides faster results. It will be possible to perform the COVID-19 test more rapidly and with less impact on the environment if MEMS sensors can replace these existing testing methods. MEMS sensors are very sensitive and selective sensors for detecting coronavirus. They are appropriate and promising due to their compact size, low input loss, high isolation and exceptionally low power consumption. Since these sensors have been in great demand on the market for a long time, there is no need to establish a distinctive industrial setting to manufacture them. This simply need to enhance the key components (microcantilever, electrode etc). A quicker test result can be attained by adjusting the cantilever's pull-in voltage, capacitance, and tip displacement. This method requires minimal resources; therefore, it produces less environmental pollution. MEMS Sensors have recently been developed for the detection of different viruses such as Dengue, Malaria, Zika, Chikungunya, etc. [26]–[28] The coronavirus detecting procedure is accomplished in 1-5 minutes at a very minimal cost. Furthermore, the cantilever-based MEMS sensors will not be easily damaged. As a result of these findings, MEMS sensor testing can perform as an alternative solution for coronavirus detection. Or it can be combined with the existing aiding approach. The accuracy of this test is less than RT-PCR, although it can be administered at home. Existing testing is currently under strained, so using the MEMS sensor as an alternative technique could be beneficial and if the COVID-19 testing result is positive, the virus can be quarantined to prevent it from spreading. To confirm, the user can also recheck the accuracy using the current testing technique.

As a consequence, this study focused on microcantilever-based MEMS sensors for the detection of viral diseases, specifically targeting COVID-19. Throughout the simulation, a passive layer was applied to the microcantilever. Key parameters such as optimal temperature, Young's modulus, Poisson's ratio, frequency spectrum, capacitance, arc length, pull-in voltage, and tip displacement were analyzed and simulated to evaluate the sensor's efficiency. To detect the presence of the coronavirus in a COVID-19 test, an antibody layer would be applied to the microcantilever's surface. If the coronavirus is identified on this layer, a specific detection device would emit a signal.

## II. DEVICE STRUCTURE AND MODELING

### A. Device Structure

A cantilever is a stiff framed structure that spreads horizontally but it is only sustained at one end. Usually, it extends from a vertical level surface toward which it must be adequately attached. A cantilever structure can be built in the form of a single-edge clamped beam. In this simulation, a microcantilever beam design was used. To develop a microcantilever model out of a diverse range of materials while maintaining exact measurements of its length, width and beam thickness. The

movement and reaction of the microcantilever were also affected by material properties such as density, thermal conductivity, elasticity or stiffness, durability, malleability and so on.

The shape of a microcantilever model is shown in Fig. 2 (a). The proposed microcantilever has three operable or detectable layers. According to this design, it implies one antibody layer, one active layer and one passive layer (non-piezoelectric layer). For the active layer, lead zirconate titanate has been used. Because the material matched the antibody adequately, the same active layer was applied for all simulations. The passive layer was built using a variety of non-piezoelectric materials (nickel, molybdenum and gold) with differing Young's modulus and Poisson's ratios. The length and width of the microcantilever beam are  $300\mu\text{m}$  and  $20\mu\text{m}$ . To achieve a reduced pull-in voltage, the material of the passive layer was changed many times. It has a thickness of  $2\mu\text{m}$ . It has a fixed one end, but the rest of it can be moved throughout easily. The microcantilever beam is enclosed in an airtight container that is totally sealed off from the outside surroundings. A grounded gold electrode is located on the enclosure's bottom side. Charge density bends the microcantilever by minimizing the spacing between the beam and the buffer layer shown in Fig. 2 (b). The buffer layer reduces absorption losses and carries electrons released by the absorber to the electrode. It hits the ground once the electrostatic force (push or pull on something while avoiding physical contact with it) beats the stress force (force per unit area) at the optimal pull-in voltage, temperature and frequency. Between the bottom of the cantilever beam and the grounding surface, there is an apparent difference (Tip Displacement) of  $2\mu\text{m}$  in this model, which assumes a thick air layer below and on each side of the support beam. The amount of the electrostatic force is directly proportional to the amount of the applied voltage. As the force is increased, deflection also increases. For the pull-in voltage, the beam finally makes contact with the ground. The Electromechanics Multiphysics interface conducts the required conversions and it also provides smoothing algorithms that regulate the movement of the atmospheric domain's mesh. The cantilever is attached to a terminal for electricity with a bias potential. Bias is the controlled discharge of direct current (DC) between two terminals to regulate the circuit. The terminal configuration changes the system capacitance automatically.

### B. Modeling

MEMS sensor is an electromechanical device designed by nanoscale technology and concentrated on the analysis, perception and detection of particular bioactive molecules among individuals. They require a minimal DC supply, negligible loss and isolation defined by the coupling capacitance between electrodes when it is activated [29]. Due to their narrow bandwidth, higher cut-off frequency, compact size and lightweight MEMS sensors can combine RF circuits and components on a microchip [30]. One of the components of this MEMS sensor is a microcantilever, which is placed into it. Microcantilever is incredibly thin and bendable with a tiny force. In this paper, we tested the effectiveness of the microcantilever which was chosen because of its leverage of direct physical contact between metals with a reduced contact resistance to produce lower input losses

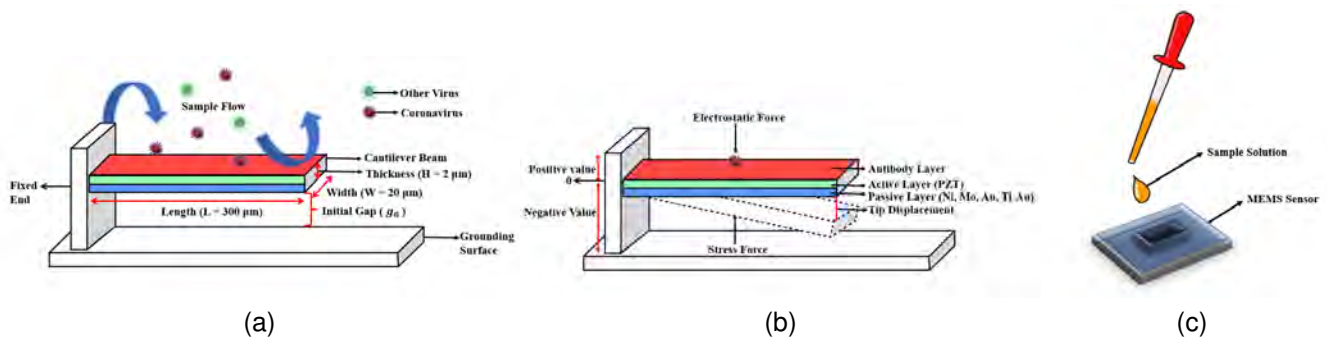


Fig. 2. (a) Geometry, (b) movement and (c) application process of the sample solution to the MEMS sensor's surface.

while operating. Antibodies are made using recombinant DNA technology. The phases in this technology include collecting genetic material from host (Human) species, splitting the DNA with restriction enzymes, linking segments with DNA ligase, injecting the recombinant DNA into the host organism and finally screening and testing transformed cells. It needs to have a surface concentration between  $0.27$  and  $4.5g/L$  [31]. They are developed based on different coronavirus variants (Omicron, Delta and Alpha) [32]–[34].

Corona virus testing procedure flowchart is shown in Fig. 3. Two ways of the sample application procedure are displayed: a nasal swab test and a patient's breath test. Two possible outcomes can occur when the liquid solution or breath is applied to the antibody layer. The response is activated and the corona virus is detected if the surface tension changes, the MEMS sensor's switch is closed and the external detection circuit is turned on. There is no reaction and no sign of the corona virus if the surface tension is not changed, the MEMS sensor's switch is opened and the external detecting circuit is switched off.

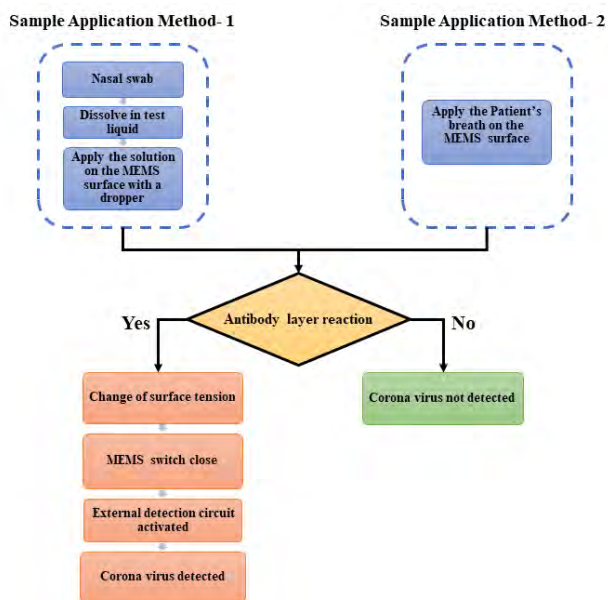


Fig. 3. Flowchart for corona virus testing method.

To avoid other viruses from being gathered by this antibody layer, only coronavirus antibodies need to be used to create it.

The device needs to be kept at  $295.15$ – $310.15$  K temperature since antibodies will denature upon drying or exposure to ambient conditions. The required pH range for the solution (buffer) is  $7.35$  to  $7.45$ . This issue of denaturation can be avoided by not preserving the antibody at high temperature (over  $338.15K$ ), because extreme heat can disturb the natural structure of both the antibody and buffer components. Naturally, coronavirus antibody has no side effects. However, some patients (pregnant women or breastfeeding mothers) may experience headaches, low blood pressure or dizziness. In order to collect samples, this method needs three stages. Initially, samples should always be gathered from the patient using a nasal swab test. This procedure usually takes a minute to complete. In the second stage, the patient swab sample needs to be dissolved in the test liquid and can be collected using a small dropper. The test liquid needs to have  $99.7\%$  saline solution mixed with Sodium azide. In the third stage, a drop of the sample solution needs to be applied to the MEMS sensor's surface. The sample solution enters through the MEMS sensor and the coronaviruses in the sample solution fall on the surface of the microcantilever, as seen in Fig. 2 (c). As an alternative to nasal samples, the patient's breath can be used. Due to the method's high sensitivity, breath carries enough viruses to be identified considering its lower viral load. Following that, the contact between the coronavirus and the antibody layer will change the surface tension and will allow the microcantilever beam to make contact with the grounding surface, as illustrated in Fig. 4. After only 3-5 minutes of analysis, the result can be visible on a simple reader device and digitally decoded as a signal. When the circuit becomes closed, an externally connected LED can be used to show the positive or negative result. Furthermore, this method has the advantage of immediately detecting the coronavirus and demanding less pull-in voltage.

For optimal COVID-19 testing results, the microcantilever's pull-in voltage, frequency and capacitance must be examined. Pull-in voltage is the mandatory voltage to activate a MEMS sensor. The accuracy of the test results increases as the pull-in voltage decreases, as well as the durability and capacitance of the beam material improve as the frequency and applied voltage decrease. If all of the parameters are followed as described above, more precise results can be obtained. Equation 1 presents the pull-in voltage (bending dominated) solution for a microcantilever beam [35].

$$V_p = \sqrt{\frac{4C_1 B}{\epsilon_P L^4 \frac{2}{C_2} (1 + C_3 \frac{g_0}{W})}} \quad (1)$$

$$B = \hat{E} H^3 g_0^3 \quad (2)$$

Where,  $C_1 = 0.07$ ,  $C_2 = 1.00$  and  $C_3 = 0.42$  are constants,  $\epsilon_P$  represents permittivity of free space,  $L$  denotes the beam's extent,  $W$  shows width,  $B$  is the phase angle,  $g_0$  is an initial gap between the beam and ground surface,  $\hat{E}$  is the young's modulus and  $H$  is the thickness of microcantilever beam.

While calculating the composite beam, every layer's Young's modulus should be calculated. It is a mechanical parameter that assesses the tensile or compressive rigidity of a solid material when a longitudinal force is exerted [35].

$$E_e = \sum \frac{E_n t_n}{t} \quad (3)$$

Fig. 4 depicts three distinct layers. Where  $E_n$ ,  $t_n$  are Young's modulus and thickness of each layer respectively ( $n = 1, 2, 3$  for the successive layers) and  $t$  is the total thickness of the composite beam.

Poisson's Equation is used to measure the static electricity of a material. It governs the electromagnetic environment inside the air and the beam [35].

$$-\Delta \cdot (\epsilon \Delta V) = 0 \quad (4)$$

Where,  $\Delta V$  is the voltage difference. The electrostatic force is the attraction or repulsion of two electrically charged entities [36].

$$F = \frac{K[q_1 \times q_2]}{D^2} \quad (5)$$

Where,  $q_1$  and  $q_2$  are two electrically charged entities and  $K$  denotes the Coulomb's constant.

Maxwell's stress force defines the force concentration exerted on the beam's emitter [37].

$$\vec{F}_{es} = -\frac{1}{2}(\vec{E} \cdot \vec{D})n + (n \cdot \vec{E})\vec{D} \quad (6)$$

Where,  $\vec{E}$  and  $\vec{D}$  are the electric field and displacement directions respectively and  $n$  is the boundary's outward standard direction.

Sensitivity is represented by [7],

$$S = \frac{\Delta output}{\Delta input} \quad (7)$$

### III. RESULTS AND DISCUSSIONS

A variety of non-piezoelectric materials are applied to construct the microcantilever in the Finite-Difference Time-Domain (FDTD) method. In this study titanium (Ti), nickel (Ni), molybdenum (Mo) and gold (Au) materials are used on the passive layer of the microcantilever. The pull-in voltage and frequency were determined depending on the type of materials. In this circumstance, the temperature is set to 77°F (Room temperature) and the initial pull-in voltages of each material are taken at 7V. Temperature fluctuations can affect the accuracy

of COVID-19 testing; thus, room temperature is preferable. This voltage has been changed based on the material type. The resonance frequency of nickel is 10KHz, gold is 14KHz and molybdenum is 50KHz. The following are the standard values [38]–[40]. The microcantilever is connected to a voltage input, while the chamber's base is neutralized. According to the simulation, the pull-in voltage seems to be the actuation voltage at which the barrier between the microcantilever and the buffer layer is reduced.

Based on equation 1, nickel has pull-in materials, each having its own Young's modulus and Poisson's voltage of 6.1333V, molybdenum has 6.4V and gold has 5.49V. The microcantilever has been constructed of three different ratios. The Young's modulus of nickel, molybdenum and gold obtained from equation 3 is 190GPa, 315GPa, and 79GPa respectively. The ratio of nickel, molybdenum and gold Poisson are considered as 0.305, 0.29, and 0.415 correspondingly. Throughout this simulation, the length, width and thickness of the microcantilever are kept constant.

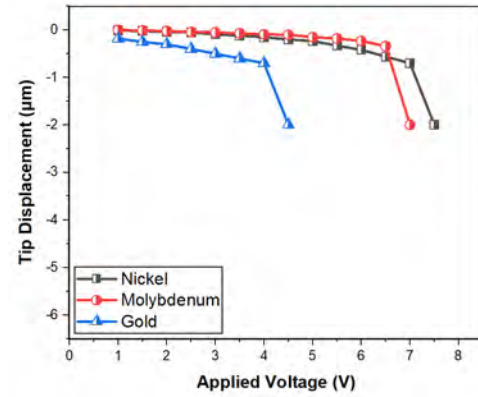


Fig. 4. Displacements of microcantilever tips as a function of applied voltage.

In a variety of materials, Fig. 4 depicts the displacement of the cantilever tip as a result of applied voltage. This MEMS sensor can determine the height, width and thickness of coronavirus by analyzing the tip displacement. It reduces as the applied voltage of the material increases. In terms of tip displacement stability, gold required a lower applied voltage than other materials. After a specific voltage, the tip displacement of the gold decreases rapidly.

Fig. 5 depicts the changes in microcantilever movement for various voltages applied to the microcantilever, as indicated by the lines on the symmetrical border. The solution does not converge when the electric field distribution increases. Following this analysis, the pull-in voltages for nickel, molybdenum and gold are 6.1333V, 6.4V and 5.49V respectively. As previously stated, lower pull-in voltage has become the key challenge for MEMS sensor durability. After analyzing conventional materials, which observed gold is performing better because it increases the sensitivity of the MEMS sensor, decreases the pull-in voltage and increases the capacitance. During this simulation period, the frequency and temperature were set by the established parameters. Gold is a very malleable metal. Each gold atom's nucleus has 79 protons. It has an atomic mass of 196.967 and an atomic radius of 0.1442nm. The density of

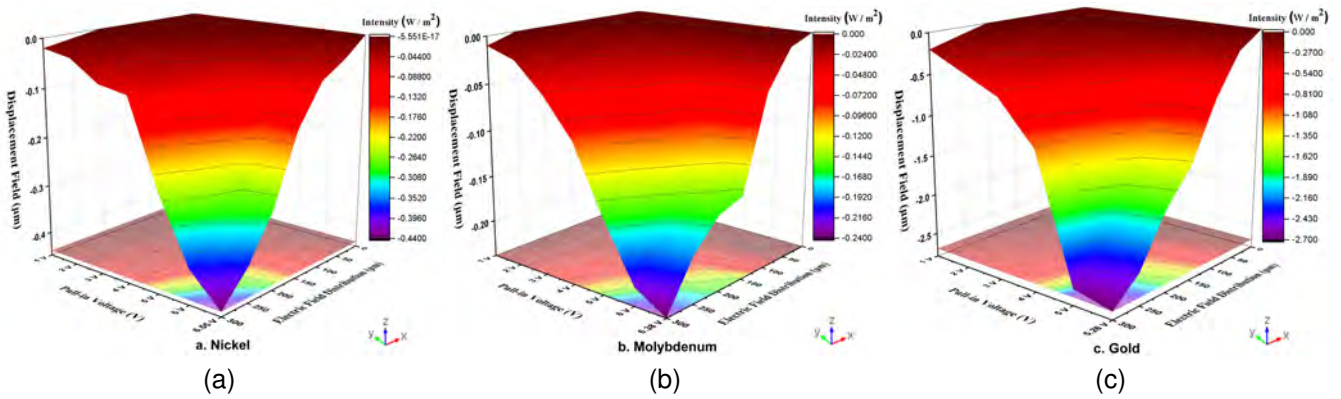


Fig. 5. Displacement field of the bottom surface of the microcantilever along the symmetrical boundary for different values of arc length.

gold is  $19,300\text{kgm}^{-3}$ . In order to further enhance the strength, accuracy and efficiency, while simultaneously reducing the pull-in voltage, it is essential to choose a cost-effective material for the development of the microcantilever.

Following thorough testing can conclude that combining titanium with gold would offer better outcomes than other gold alloys named gold aluminum (aluminium and gold), rose gold (copper and gold) and white gold (nickel, palladium or platinum and gold). Titanium-gold (Ti-Au) is a metallurgical alloy composed of " $\beta$  Ti3Au" (beta-titanium 3 gold). In terms of productivity, strength, structural stiffness, durability and magnetism; Ti-Au outperformed their basic metals (Gold and Titanium). It has been reported that a titanium-gold alloy is up to four times stronger than pure titanium [41]. The purpose of using a strong material for the microcantilever is because of its longevity, robustness and stability.

electric charge. The COVID-19 test's accuracy would improve as capacity increased. The accuracy is essential to determine the test's potential to identify between unhealthy and healthy conditions.

Fig. 7 depicts the changes in Ti-Au microcantilever movement for voltages applied to that cantilever, as indicated by the lines on the symmetrical border. The displacement field diminishes as the arc length increases. During this simulation period, the temperature was set at  $77^\circ\text{F}$  ( $298.15\text{K}$ ,  $RT$ ). The length, width and thickness of the cantilever remain unchanged. According to equations 3 and 4, Ti-Au has a Young's modulus of  $112\text{GPa}$  and a Poisson's ratio of 0.33.

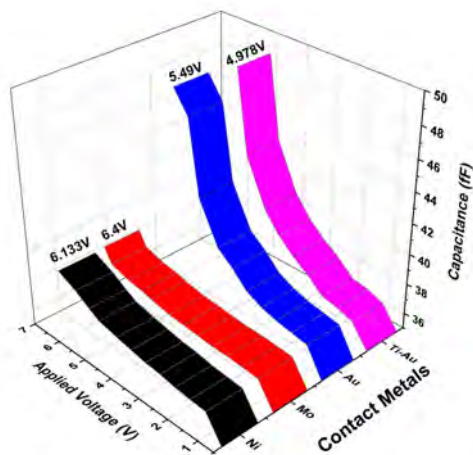


Fig. 6. Capacitance vs Applied voltage for different cantilever materials.

Fig. 6 shows the anticipated DC C-V curve for the microcantilever beam. The suitable length, width and thickness for each material are  $300\mu\text{m}$ ,  $20\mu\text{m}$ , and  $2\mu\text{m}$ , accordingly. These simulations are done at ambient temperature ( $77^\circ\text{F}$ ). Here capacitance rises as the applied voltage increases. As shown above, Ti-Au has a lower applied voltage but a higher capacitance ( $49\text{fF}$ ). More capacity is required to hold more

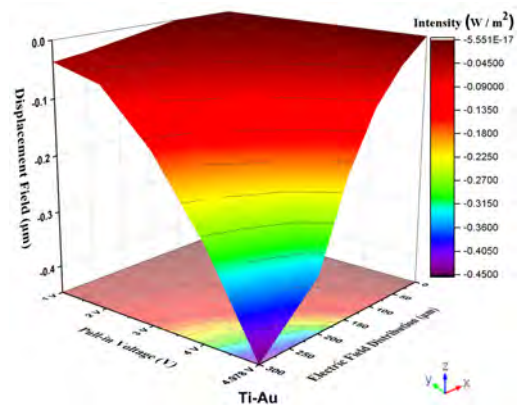


Fig. 7. Displacement field of the bottom surface of the Ti-Au microcantilever along the symmetrical boundary for different values of arc length.

From Fig. 8 can see that, the pull-in voltage of both gold and Ti-Au was  $7\text{V}$ . Using equation 1, can calculate the pull-in voltage of gold ( $5.26\text{V}$ ) and Ti-Au ( $4.978\text{V}$ ). Ti-Au has a lower pull-in voltage than gold. As an outcome, the Ti-Au microcantilever is ideal for the COVID-19 test due to its lower pull-in voltage and effectiveness.

Ti-Au has a substantially higher density ( $4540\text{kgm}^{-3}$ ) than titanium and is less expensive than a gold microcantilever. Because of its robustness, Ti-Au is an easy-to-maintain metal. The minimal input of structural properties required to produce a detectable output change is defined as a sensor's sensitivity. Equation 7 is used to calculate the contact metals' sensitivity.

TABLE I  
COMPARISON OF THE PROPOSED MODEL WITH THE PREVIOUS STUDIES

Reference	Detection Technique	Tested Sample	Material	Target	Detection Time	Temperature (°F)	Density (kg/m <sup>3</sup> )	Sensitivity
Ref [42]	Electro-chemical	Not recorded	PANI	Nucleic Acid	1 h	98.6	1100	High
Ref [43]	MEMS Sensor	Nasal swabs	Gold	SARS-CoV-2 virus	40 min	74	19300	Low
Ref [44]	Optical (P-FAB)	PBS Buffer	Gold	N-Protein	10 min	Not Recorded	19300	Not Recorded
Ref [45]	Optical Electro-chemical	Nasal swab, blood sample	Hybrid nano-material	N-Protein	35 min	77	Not Recorded	High
Ref [46]	MEMS Sensor	Not Recorded	Piezo-electric material	S-protein	Not Recorded	Not Recorded	Not Recorded	Not Recorded
Proposed	MEMS Sensor	Nasal swab/ breath sample	Ti-Au	SARS-CoV-2 virus	3-5 min	77	4540	High

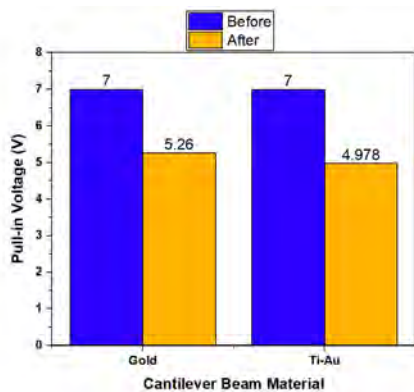


Fig. 8. Pull-in voltage of Gold and Ti-Au before and after applying the sample.

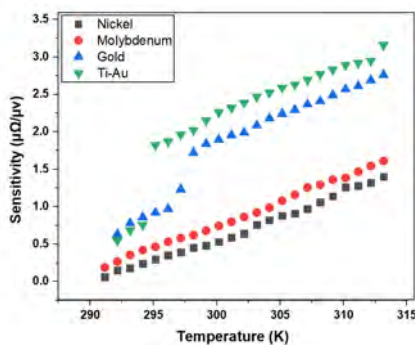


Fig. 9. Temperature against sensitivity for Ni, Mo, Au and Ti-Au microcantilevers.

Fig. 9 depicts the relationship between microcantilever temperature and sensitivity for Ni, Mo, Au and Ti-Au microcantilevers. The result indicates that when the temperature rises, the sensitivity also rises. This is a positive development. Ti-Au is suitable for this study since it has the highest sensitivity of all. In this situation, temperatures between room temperature and body temperature (295.15–310.15 K) are considered acceptable.

Numerous doctors and researchers have used MEMS biosensors for diagnostic purposes. Remarkable progress has been made in the implementation of MEMS cantilever sensors for precise detection and progressive observation of blood pressure, HIV and Hepatitis (A, B, and C) viruses [47]–[49]. The micrometer-sized cantilever offers the possibility of creating an extremely sensitive sensor. Inspiration from the previous excellent work led to an exploration of MEMS sensors.

Table I presents a comparison between previous research studies using various types of biosensor detection techniques and the one that is being proposed. As device materials, the studies used PANI, gold, hybrid nanomaterial and piezoelectric material. Optical and electrochemical detection methods for biosensors are often more sensitive, although they also have certain limitations. Such as, [42] having a limited temperature range, requiring a significant amount of time to obtain optimal results and demanding high-quality laboratory. Reference [44] requiring pricey expenses and a facility where ambient light can not affect the operation. Additionally, [45] presents high-cost concerns, light sensitivity, a limited temperature range, a lengthy time for optimal results, and a requirement for suitable laboratory and qualified personnel. According to the comparison table, the MEMS Sensor detection technique required room temperature. Reference [43] requires a longer detection time, lower sensitivity issue, has a limited number of clinical samples and is insensitive in effluent samples. In [46] the provided analysis lacks precision in clarifying the concepts of temperature, detection time and sensitivity. In the proposed model, using a Microcantilever-based MEMS sensor substantially decreased the coronavirus detection time (3 – 5min) and gave the higher sensitivity. Previous research has not looked at the topic of material capacitance. To store more electric charge, greater capacity is needed. COVID-19 test's precision improves as capacity increases. The test's ability to distinguish between hazardous and healthy situations depends on its accuracy. However, this research places particular emphasis on this aspect, specifically the capacitance of Ti-Au, which is measured to be

49 fF. One drawback associated with the proposed model is its limited temperature range for preservation, which spans from 295.15K to 310.15K. The limitation of this work is relatively minor in comparison to other studies. In addition, this proposed model is performing superior concerning other researchers' output.

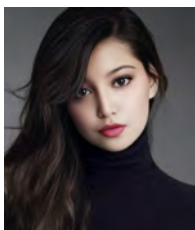
#### IV. CONCLUSION

The COVID-19 pandemic, caused by the SARS-CoV-2 virus, has highlighted the urgent need for rapid and accurate diagnostic tools. This research presents the design and simulation of a microcantilever-based MEMS sensor capable of detecting COVID-19 within a temperature range of 295.15 K to 310.15 K. Our simulations demonstrate that a Ti-Au microcantilever offers superior sensitivity, faster testing times, and a higher capacitance of 49 fF compared to other materials. The lower pull-in voltage of the Ti-Au microcantilever (4.978 V) reduces the required electrostatic actuation voltage, making it a more effective choice for COVID-19 detection. While this study focuses on COVID-19, the proposed MEMS sensor design has potential applications for detecting a broader range of viral and bacterial pathogens. Future research could explore the sensor's sensitivity and specificity for detecting other respiratory viruses, such as influenza and respiratory syncytial virus (RSV). Additionally, investigating the sensor's performance in real-world clinical settings would be crucial for validating its practical utility.

#### REFERENCES

- [1] A. Ullah, A. Tareq, A. Naziba, M. Khalil, M. Nafisa, H. Alam, A. Intiaz, and A. Kibria, "Uranium determination in water, soil and stone through adsorptive accumulation of u (vi)-chloranilic acid complex," *NUCLEAR SCIENCE AND APPLICATIONS*, vol. 27, no. 1&2, 2018.
- [2] M. Sharkar, A. T. Naziba, M. T. Nafisa, and A. H. M. Shatil, "Load factor optimization with different algorithm."
- [3] A. T. Naziba and M. N. Uddin, "Non-invasive heat-induced numerous tissue ablation using high intensity focused ultrasound technique," *AJSE*, vol. 21, no. 2, pp. 89–97, 2022.
- [4] A. T. Naziba, M. T. Nafisa, and M. N. Uddin, "Cyclic olefin copolymer based photonic crystal fiber as single mode thz waveguide," *International Journal of Computing and Digital Systems*, vol. 15, no. 1, pp. 271–278, 2024.
- [5] A. T. Naziba and M. N. Uddin, "Simulation of high intensity focused ultrasound device in healthcare application for non-invasive heat induced tissue ablation," in *Proceedings of the 2nd International Conference on Computing Advancements*, 2022, pp. 473–477.
- [6] A. T. Naziba, M. H. Mahmud, M. T. Nafisa, S. A. Rahman, and M. N. Uddin, "Design and simulation of a pcf-spr biosensor for enhanced blood cancer detection," in *2024 IEEE International Conference on Signal Processing, Information, Communication and Systems (SPICSCON)*. IEEE, 2024, pp. 1–4.
- [7] A. T. Naziba and M. N. Uddin, "Cancer cell detection biosensor utilizing dual-core pcf-based surface plasmon resonance," in *2024 Third International Conference on Distributed Computing and Electrical Circuits and Electronics (ICDCECE)*. IEEE, 2024, pp. 1–5.
- [8] S. Chakraborty, I. S. Bristy, A. T. Naziba, M. R. Rahman, and M. N. Uddin, "An empirical analysis of 5.4 thps mdm-wdm hybrid network for 100km multimode communication using multimode optical fiber," in *2024 IEEE International Conference on Power, Electrical, Electronics and Industrial Applications (PEEIACON)*. IEEE, 2024, pp. 134–139.
- [9] A. T. Naziba, S. Chakraborty, and M. N. Uddin, "Single mode thz waveguide using zeonex-based photonic crystal fiber," in *2024 IEEE International Conference on Power, Electrical, Electronics and Industrial Applications (PEEIACON)*. IEEE, 2024, pp. 685–689.
- [10] A. T. Naziba, M. T. Nafisa, R. Sultana, M. F. Ehsan, A. Tareq, R. Rashid, H. Das, A. A. Ullah, and A. F. Kibria, "Structural, optical, and magnetic properties of co-doped zno nanorods: Advancements in room temperature ferromagnetic behavior for spintronic applications," *Journal of Magnetism and Magnetic Materials*, vol. 593, p. 171836, 2024.
- [11] F. Islam, A. T. Naziba, M. R. Rahman, and M. N. Uddin, "Performance analysis of 3.75 gbit/s secure sac-ocdma-wdm-fso system by using the and subtraction technique," in *2024 International Conference on Electrical, Communication and Computer Engineering (ICECCE)*, 2025.
- [12] M. H. Mahmud, M. T. H. Nayan, D. M. N. A. Ashir, and M. A. Kabir, "Software risk prediction: systematic literature review on machine learning techniques," *Applied Sciences*, vol. 12, no. 22, p. 11694, 2022.
- [13] M. H. Mahmud, A. T. Naziba, F. Islam, M. T. Nafisa, S. A. Rahman, and M. N. Uddin, "Enhanced breast cancer detection using pcf-spr sensor: A machine learning approach," in *2024 International Conference on Recent Progresses in Science, Engineering and Technology (ICRPSET)*. IEEE, 2024, pp. 1–4.
- [14] M. H. Mahmud, A. H. Maruf, and M. N. Uddin, "Ultra-fast core mode prediction in plasmonic crystal fiber sensor: A machine learning approach," in *2024 International Conference on Innovations in Science, Engineering and Technology (ICISET)*. IEEE, 2024, pp. 1–6.
- [15] S. Abbasi and Ç. Sıcakyyüz, "A review of the covid-19 pandemic's effects and challenges on worldwide waste management for sustainable development," *International Journal of Environmental Science and Technology*, pp. 1–30, 2024.
- [16] B. Hu, H. Guo, P. Zhou, and Z.-L. Shi, "Characteristics of sars-cov-2 and covid-19," *Nature Reviews Microbiology*, vol. 19, no. 3, pp. 141–154, 2021.
- [17] J. Saniasiaya, M. A. Islam, and B. Abdullah, "Prevalence of olfactory dysfunction in coronavirus disease 2019 (covid-19): a meta-analysis of 27,492 patients," *The Laryngoscope*, vol. 131, no. 4, pp. 865–878, 2021.
- [18] A. A. Agyeman, K. L. Chin, C. B. Landersdorfer, D. Liew, and R. Ofori-Asenso, "Smell and taste dysfunction in patients with covid-19: a systematic review and meta-analysis," in *Mayo Clinic Proceedings*, vol. 95, no. 8. Elsevier, 2020, pp. 1621–1631.
- [19] M. Liu, Q. Li, J. Zhou, W. Ai, X. Zheng, J. Zeng, Y. Liu, X. Xiang, R. Guo, X. Li *et al.*, "Value of swab types and collection time on sars-cov-2 detection using rt-pcr assay," *Journal of virological methods*, vol. 286, p. 113974, 2020.
- [20] G. Lippi, A.-M. Simundic, and M. Plebani, "Potential preanalytical and analytical vulnerabilities in the laboratory diagnosis of coronavirus disease 2019 (covid-19)," *Clinical Chemistry and Laboratory Medicine (CCLM)*, vol. 58, no. 7, pp. 1070–1076, 2020.
- [21] P. M. Thwe and P. Ren, "Analysis of sputum/tracheal aspirate and nasopharyngeal samples for sars-cov-2 detection by laboratory-developed test and panther fusion system," *Diagnostic Microbiology and Infectious Disease*, vol. 99, no. 1, p. 115228, 2021.
- [22] L. Shen, S. Cui, D. Zhang, C. Lin, L. Chen, and Q. Wang, "Comparison of four commercial rt-pcr diagnostic kits for covid-19 in china," *Journal of Clinical Laboratory Analysis*, vol. 35, no. 1, p. e23605, 2021.
- [23] D. Ferrari, E. Sabetta, D. Ceriotti, A. Motta, M. Strollo, G. Banfi, and M. Locatelli, "Routine blood analysis greatly reduces the false-negative rate of rt-pcr testing for covid-19," *Acta Bio Medica: Atenei Parmensis*, vol. 91, no. 3, p. e2020003, 2020.
- [24] A. Stang, J. Robers, B. Schonert, K.-H. Jöckel, A. Spelsberg, U. Keil, and P. Cullen, "The performance of the sars-cov-2 rt-pcr test as a tool for detecting sars-cov-2 infection in the population: A survey of routine laboratory rt-pcr test results from the region of münster, germany," *medRxiv*, pp. 2021–05, 2021.
- [25] A. M. Shrivastav, U. Cvelbar, and I. Abdulhalim, "A comprehensive review on plasmonic-based biosensors used in viral diagnostics," *Communications biology*, vol. 4, no. 1, p. 70, 2021.
- [26] D. Dunuwila, Y. Amarasinghe, and W. Jayathilaka, "Design and simulation of a novel mems based microfluidic lab-on-a-chip device for dengue virus detection," in *IECON 2023-49th Annual Conference of the IEEE Industrial Electronics Society*. IEEE, 2023, pp. 1–6.
- [27] M. Katta and R. Sandanalakshmi, "Simultaneous tropical disease identification with pzt-5h piezoelectric material including molecular mass biosensor microcantilever collection," *Sensing and Bio-Sensing Research*, vol. 32, p. 100413, 2021.
- [28] A. Niranjana, P. Gupta, and M. Rajoria, "Polymer-based mems sensor for label-free chikungunya virus detection," in *Macromolecular Symposia*, vol. 407, no. 1. Wiley Online Library, 2023, p. 2200104.
- [29] G. Koley, "Editorial for the special issue on mems/nems sensors: Fabrication and application," p. 554, 2019.
- [30] M. K. Mishra, V. Dubey, P. Mishra, and I. Khan, "Mems technology: A review," *J. Eng. Res. Rep.*, vol. 4, no. 1, pp. 1–24, 2019.
- [31] E. Marklund, S. Leach, H. Axelsson, K. Nyström, H. Norder, M. Bemark, D. Angeletti, A. Lundgren, S. Nilsson, L.-M. Andersson *et al.*, "Serum-igg responses to sars-cov-2 after mild and severe covid-19 infection and analysis of igg non-responders," *PloS one*, vol. 15, no. 10, p. e0241104, 2020.

- [32] M. Eisenhut, J. I. Shin *et al.*, "Covid-19 vaccines and coronavirus 19 variants including alpha, delta, and omicron: present status and future directions," *Life Cycle*, vol. 2, 2022.
- [33] X. He, W. Hong, X. Pan, G. Lu, and X. Wei, "Sars-cov-2 omicron variant: characteristics and prevention," *MedComm*, vol. 2, no. 4, pp. 838–845, 2021.
- [34] N. Kumar, S. Quadri, A. I. AlAwadhi, and M. AlQahtani, "Covid-19 recovery patterns across alpha (b. 1.1. 7) and delta (b. 1.617. 2) variants of sars-cov-2," *Frontiers in immunology*, p. 379, 2022.
- [35] R. K. Gupta *et al.*, "Electrostatic pull-in test structure design for in-situ mechanical property measurements of microelectromechanical systems (mems)," Ph.D. dissertation, Massachusetts Institute of Technology, 1997.
- [36] Y. Zheng, M. Zhao, P. Sun, and L. Song, "Optimization of electrostatic force system based on newton interpolation method." *Journal of Sensors*, 2018.
- [37] A. Davis and V. Onoohin, "The maxwell stress tensor and electromagnetic momentum," *Progress In Electromagnetics Research Letters*, vol. 94, pp. 151–156, 2020.
- [38] Y. Park, E. J. Lee, and T. Kouh, "Field-dependent resonant behavior of thin nickel film-coated microcantilever," *Micromachines*, vol. 8, no. 4, p. 109, 2017.
- [39] C. Lee, H. Kang, C. Kim, and K. Shin, "A novel method to guarantee the specified thickness and surface roughness of the roll-to-roll printed patterns using the tension of a moving substrate," *Journal of Microelectromechanical Systems*, vol. 19, no. 5, pp. 1243–1253, 2010.
- [40] M. Teranishi, C.-Y. Chen, T.-F. M. Chang, T. Konishi, D. Yamane, K. Machida, K. Masu, and M. Sone, "Enhancement in structure stability of gold micro-cantilever by constrained fixed-end in mems devices," *Microelectronic Engineering*, vol. 187, pp. 105–109, 2018.
- [41] C. Nongthombam, S. Patani, N. D. Gulve, A. Nehete, M. P. Pardeshi, and S. Aher, "Stress evaluation of titanium-gold and titanium-aluminum-vanadium alloy for orthodontic implants: A comparative finite element model study," *Journal of Indian Orthodontic Society*, vol. 51, no. 4, pp. 245–249, 2017.
- [42] Z. Song, Y. Ma, M. Chen, A. Ambrosi, C. Ding, and X. Luo, "Electrochemical biosensor with enhanced antifouling capability for covid-19 nucleic acid detection in complex biological media," *Analytical chemistry*, vol. 93, no. 14, pp. 5963–5971, 2021.
- [43] S. A. Muhsin, Y. He, M. Al-Amidie, K. Sergovia, A. Abdullah, Y. Wang, O. Alkorjia, R. A. Hulsey, G. L. Hunter, Z. K. Erdal *et al.*, "A microfluidic biosensor architecture for the rapid detection of covid-19," *Analytica Chimica Acta*, vol. 1275, p. 341378, 2023.
- [44] M. Divagar, R. Gayathri, R. Rasool, J. K. Shamlee, H. Bhatia, J. Satija, and V. Sai, "Plasmonic fiber optic absorbance biosensor (p-fab) for rapid detection of sars-cov-2 nucleocapsid protein," *IEEE sensors journal*, vol. 21, no. 20, pp. 22 758–22 766, 2021.
- [45] Priyanka, B. Mohan, E. Poonia, S. Kumar, Virender, C. Singh, J. Xiong, X. Liu, A. J. Pombeiro, and G. Singh, "Covid-19 virus structural details: Optical and electrochemical detection," *Journal of Fluorescence*, pp. 1–22, 2023.
- [46] M. A. Bani-Hani, M. A. Al-Moghazy, W. A. Altabay, S. A. Kouritem, and M. Hakam, "Detecting technique of covid-19 via an optimized piezoelectric sensor," *JJMIE*, vol. 17, no. 2, 2023.
- [47] I. M. Serene, M. RajasekharaBabu, and Z. C. Alex, "A study and analysis of microcantilever materials for disease detection," *Materials Today: Proceedings*, vol. 5, no. 1, pp. 1219–1225, 2018.
- [48] M. Kaisti, T. Panula, J. Leppänen, R. Punkkinen, M. Jafari Tadi, T. Vasankari, S. Jaakkola, T. Kiviniemi, J. Airaksinen, P. Kostiaainen *et al.*, "Clinical assessment of a non-invasive wearable mems pressure sensor array for monitoring of arterial pulse waveform, heart rate and detection of atrial fibrillation," *NPJ digital medicine*, vol. 2, no. 1, p. 39, 2019.
- [49] A. V. Ganesan, D. K. Kumar, A. Banerjee, and S. Swaminathan, "Mems based microfluidic system for hiv detection," in *2013 13th IEEE International Conference on Nanotechnology (IEEE-NANO 2013)*. IEEE, 2013, pp. 557–560.



**Anika Tun Naziba** received her B.Sc. degree in Electrical and Electronics Engineering from Bangladesh University of Business and Technology (BUBT). She obtained her M.Sc. degree in Electrical and Electronics Engineering from American International University-Bangladesh (AIUB). She is currently researching on biomedical engineering at American International University-Bangladesh (AIUB), Dhaka, Bangladesh. Her research interests include biomedical engineering and optical fiber. She has also published multiple papers on optical fibers.



**Mahmudul Hoque Mahmud** received his B.Sc. degree in Applied Statistics from the University of Dhaka. He is currently pursuing his M.Sc. degree in the Computer Science Department at American International University-Bangladesh (AIUB), Dhaka, Bangladesh. His research interests include machine learning and optical fiber. He has also published multiple papers on machine learning and photonic crystal fibers.



**Manika Tun Nafisa** received her B.Sc. and M.Sc. degrees from American International University-Bangladesh (AIUB) in Electrical and Electronics Engineering. She is currently pursuing her Ph.D. at Kennesaw University. Her research interests include Semiconductor, Spintronics, Optoelectronics, Bioengineering, and Renewable Energy. She has also published many papers.



**S M Atiqur Rahman** received his B.Sc. degree in Electrical and Electronic Engineering from BRAC University. He is currently pursuing his Ph.D. at Kennesaw State University. His research interests include Semiconductor, Spintronics, Optoelectronics, Bioengineering, and Renewable Energy. He has also published many papers.



**Ariful Hoque Maruf** received his Bachelor of Science in Software Engineering from the University of Dhaka. He started his career as a Software Engineer Intern at Brain Station 23 and became a Senior Software Engineer (Android). Concurrently, he has been working as an Android Developer at Tise in Norway till now. His interests include Kotlin and Android development, and machine learning. He has a contest rating of 1721 (max. expert) on Codeforces.



**Md. Tanvir Hasan** received his B.Sc. and M.Sc. degrees in electrical and electronic engineering from Khulna University of Engineering & Technology (KUET), Bangladesh, in 2006 and 2007, respectively. He earned his Ph.D. in electrical and electronic engineering from the University of Fukui, Japan, in 2013. He is currently an Associate Professor with the Department of Electrical and Electronic Engineering, Jashore University of Science and Technology (JUST), Bangladesh. His research interests include the growth, design, fabrication, characterization, simulation, and modeling of III–V-based semiconductor devices (electronic and optoelectronic).



**Mohammad Nasir Uddin** received his B.Sc. in Electrical and Electronic Engineering from Khulna University of Engineering and Technology (KUET) in 2003, and an M.Sc. Engineering in Computer Networks from Middlesex University, UK, in 2006. He completed his Ph.D. from Kyushu University, Japan, in 2015. He is a Certified Professional Engineer (PEng.) from IEB Bangladesh (2017) and currently serves as a Professor in the Department of Electrical and Electronic Engineering, American International University-Bangladesh (AIUB). His current research interests include Active MMI Laser Diode, High-Speed Optical Communication, Wireless Communication, and Optical Sensor networks. Dr. Uddin is a senior member (SMIEEE) of the IEEE.